



Research Article

Environmentally Benign Green Synthesized Chitosan-pNIPAm Composite Hydrogel

Mohammad Amir Qureshi^{1*}, Nahid Nishat¹, Shakeel Ahmed^{2*}

¹Department of Chemistry, Faculty of Natural Science, Jamia Millia Islamia (Central University), New Delhi-110025, India

²Department of Chemistry, Government Degree College Mendhar, Mendhar, Jammu and Kashmir, 185211, India
E-mail: maq248@gmail.com

Received: 4 August 2022; **Revised:** 12 October 2022; **Accepted:** 21 November 2022

Abstract: To overcome the recent hassles of hydrogels like toxicity, low swelling, and less antibacterial activity, we developed silver nanoparticles (AgNPs) loaded hydrogel and tested its activity against *Escherichia coli*. Encapsulation of AgNPs into the hydrogel confirms after having peaks at $1,320\text{ cm}^{-1}$, $\sim 1,700\text{ cm}^{-1}$, $\sim 3,000\text{ cm}^{-1}$ and 770 cm^{-1} . The nanoparticles' size range was 10-15 nm and they were distributed throughout the hydrogel with unreacted plant extract. The highest inhibition zone of nanoparticle-loaded hydrogel was 15 mm, at 25 °C, pH 4.4 and the lowest was 7 mm at 37 °C, pH 9.4. Results encourage the use of developed hydrogel for biomedical applications.

Keywords: chitosan, pNIPAm, silver nanoparticles, hydrogel, antibacterial, biomedical

1. Introduction

Nanotechnology is one of the most working areas for analysis these days in the contemporary world. Nanoparticles (NPs) are the basic part of nanotechnology with a larger surface area to volume ratio [1]. Wounds of any living being are usually infected by bacteria, fungi, etc [2]. Silver nanoparticles (AgNPs) are widely known for their antimicrobial property. A bio-friendly green preparation of NPs is a fast-developing area in nanotechnology [3]. Plant-mediated AgNPs are a relatively newer concept. Recent research has exhibited that silver (Ag), in the form of green NPs, is a very productive antimicrobial agent in comparison with Ag in bulk form or Ag in the ionic form [4]. The therapeutic effectiveness of AgNPs is multi folds higher than traditional Ag forms. The green method is the easiest method to synthesize AgNPs from plant extract [5, 6].

Hydrogels, a polymeric network, have the capacity to contain large amounts of water (H₂O) without losing their shape [7]. They are very encouraging for medical applications and they have great prospects of use in wound care, contact lenses, drug delivery vehicles, etc. Chitosan (CS), a natural polymer, is one of the most plentiful nitrogen-containing polysaccharides with listed a wide range of applications in biomedical fields and the pharmaceutical industry [8]. It has to be highlighted here that there is a number of polymers being applied with medicinal hydrogels, and poly (N-vinyl pyrrolidone) (PVP) is one of them [9]. PVP is a market-available biocompatible polymer. Among smart polymers, poly (N-isopropylacrylamide) (pNIPAm), has been widely examined due to its unique phase separation at 32 °C [10].

In this article, the green AgNPs are analyzed extensively with properties noteworthy to recent existing

developments. Contrasting from the previous work [11], we study the absorption of AgNPs by hydrogel films at different temperatures and pH 4.4, 7.4 and 9.4 in ambient temperature. Transmission electron microscopy (TEM) and ultraviolet (UV) analysis were used to check the size and shape of green AgNPs. Fourier transform infrared spectroscopy (FTIR) and field-emission scanning electron microscopy (FESEM) are used to assess the encapsulation of AgNPs into the hydrogel film. Finally, AgNPs loaded hydrogel film will be tested against *Escherichia coli* in antibacterial analysis by disc diffusion method for the relative outcome. This study will be helpful to use green AgNPs loaded hydrogel for biomedical applications [12, 13].

2. Materials and methods

2.1 Materials

PVP supplied from Sigma-Aldrich Chemical (United States) with molecular weight, MW = 1,400-1,600 g/mol. CS powder (Aldrich Chemical), MW = 161,000 g/mol, degree of deacetylation, DD = 75.6%, 200-400 mPa.s 1% (w/v) of polymer in aqueous acetic acid (CH₃COOH) solution was used without further purification. pNIPAm purchased from Sigma-Aldrich Chemical (United States). Silver nitrate (AgNO₃) (99.5%) was purchased from Merck Specialties Private Limited. The bacterial strain, *E. coli* SN-1224, has been received from Holy Family Hospital, New Delhi-110025, India.

2.2 Preparation of leaf extract

Salix alba is an Indian medicinal plant collected from Jammu and Kashmir, India. Garden-fresh leaves of *S. alba* were stockpiled and washed rigorously initially with ground H₂O then by distilled H₂O to wash out dust particles and dried at 25 °C. About 50 g of *S. alba* crushed leaves were transferred into a 500 ml round bottom flask containing 500 ml of distilled H₂O and boiled for one hour. The settled extracts were then filtered, three times, by using Whatman filter paper No. 1. The filtered extract was then refrigerated for further analysis.

2.3 Preparation of AgNPs

AgNO₃ of concentration 0.01 mol/dm³ was prepared in an Erlenmeyer flask, then 1 ml, 3 ml and 5 ml of *S. alba* leaf extracts were added separately into 15 ml of AgNO₃ solution, keeping its concentration at 0.01 mol/dm³. One ml of cetrimonium bromide (CTAB), as a stabilizing agent, was added to the same solution, keeping its concentration at 0.05 mol/dm³. Reduction of Ag ions was observed by recording the absorbance of the mixture between 300-800 nm by using a UV-visible (UV-Vis) spectrophotometer. The formation of NPs was also confirmed with a change in the color of the solution from pale yellow to dark brown.

2.4 Loading of AgNPs into the chitosan-pNIPAm (CP1) hydrogel

Optimization of chitosan-pNIPAm (CP1) hydrogel has already been discussed in our previous work [11]. CP1 hydrogel dipped into each green AgNPs colloidal solution of pH 4.4, 7.4, 9.4 at 25 °C, 37.3 °C and 45 °C temperatures. After 24 hours, AgNPs loaded chitosan-pNIPAm hydrogel (CPAg) hydrogel from every solution was picked up and refrigerated for further testing. Figure 1 showed the AgNPs loaded CPAg hydrogel at 37 °C and 25 °C temperatures. AgNPs were not stable at 45 °C. So, sample preparation for further analysis at 45 °C was not feasible.

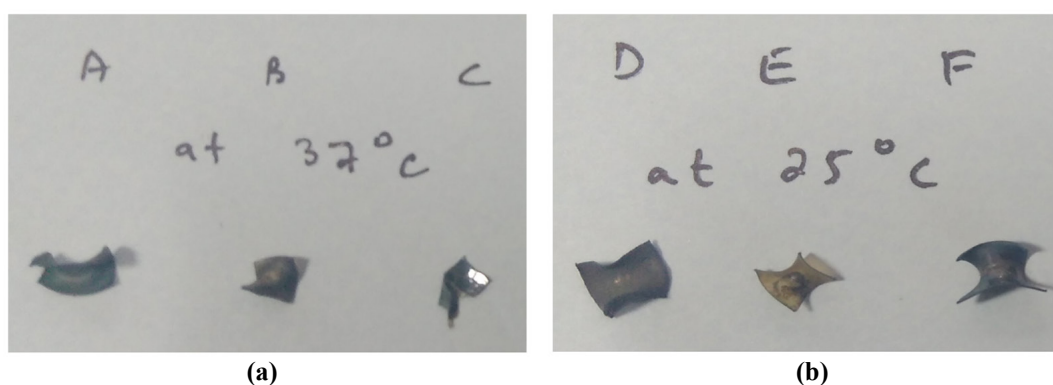


Figure 1. Images of AgNPs loaded CPAg films at 37 °C and 25 °C. A and D are for acidic, B and E are for basic and C and F are for neutral; colloidal solutions of AgNP

2.5 Swelling analysis

For H₂O uptake measurements, all the small pieces of chitosan/pNIPAm (CP) hydrogels with an optimized ratio of 4:1 with a variable amount of pNIPAm were weighed (W_d) before being immersed in phosphate buffer solution (PBS) solution of pH 4.4, 7.4 and 9.4 at 25 °C and 37 °C temperature. After dipping for different time intervals, hydrogels were cautiously picked up from the PBS solution. Removing excess H₂O from the surface, then they were weighed to know the swollen weight (W_s) as a function of the dipping time. The swelling kinetics of hydrogels was determined by the below formula:

$$\text{Swelling\%} = \frac{W_s - W_d}{W_d} \times 100$$

where W_s and W_d are the weight of the swollen hydrogel and dry hydrogel.

2.6 Characterization

UV-Vis spectrophotometer (UV-1800, Shimadzu, Japan) was employed to examine the reduction of silver ions by *S. alba* leaves extract between 200-800 nm. FTIR (Vertex 70v, Bruker, France) was used to detect the presence of particular functional groups of CPAg hydrogel and record the changes taking place after the encapsulation of AgNPs into the hydrogel. The range of scans was 4,000 to 650 cm⁻¹. TEM, operated at an accelerated voltage of 120 kV, analyzed the particle size and morphology while the morphology of the CPAg hydrogel was observed by FESEM (Nova NanoSem SEM, FEI, Netherland). Antibacterial analysis of CPAg hydrogel was performed by disc diffusion against *E. coli* to check its effectiveness as an antibacterial agent.

3. Results and discussions

This study is the development of green AgNPs loaded CS-pNIPAm hydrogel for biomedical applications like wounds, acne, burns, etc. In this work, we tried to observe the effects of NPs that are loaded into the hydrogel at different temperatures and different pHs. Synthesis of green NPs will be analyzed by UV-Vis and TEM. Their encapsulation will be examined from changes in FTIR peaks of hydrogel and FESEM images. In last, in-vitro antibacterial analysis through disc diffusion will show the effective release of green AgNPs form hydrogel.

3.1 Swelling analysis

Optimization and swelling analysis of developed hydrogels has already been reported by us [11]. Here, we summarize the key points of swelling of optimized hydrogel. The CS hydrogel was weak in strength and was pH sensitive. So, pNIPAm was added to make it temperature sensitive as well. The 4:1 ratio of 3% CP hydrogel was optimized which was high in CS amount. The swelling of optimized hydrogel was checked at pH 4.4, 7.4, 9.4 and 25 °C and 37 °C temperature of PBS solutions. At low temperatures and pH 9.4, the swelling was low. The effect of pNIPAm concentration on swelling was also measured. At high pNIPAm content at 25 °C, pNIPAm becomes hydrophilic and recorded low swelling due to high crosslinking in the hydrogel. A decrease in swelling takes place after attaining a peak, it may be due to the leaching of glycerol. At 37 °C, low swelling was observed, it was because of pNIPAm changes into a hydrophobic phase from hydrophilic. The same procedure was followed for swelling analysis at pH 7.4 at 25 °C and 37 °C temperature. The swelling was high at pH 7.4 because the above factors work less in these conditions. At pH 4.4, the swelling was very high and hydrogel became very weak.

3.2 UV-Vis studies

AgNPs seem pale yellow-brown as a consequence of the surface plasmon resonance (SPR) peak [14]. Leaves extracts of *S. alba* mixed in AgNO₃(aq) solution, the color of the mixture changes from pale yellow to dark brown signifying the reduction of AgNO₃ into AgNPs. Similar changes were also reported in previous studies [15] to confirm the reaction of extract and AgNO₃. UV-Vis spectra of an optimized sample are displayed in Figure 2.

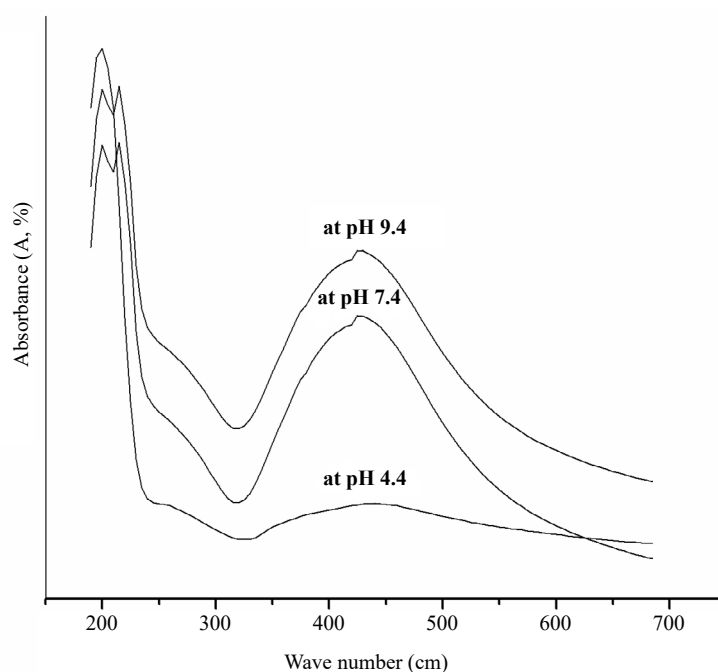


Figure 2. UV-Vis spectra of Ag nanoparticles at different pH's

Absorption spectra of AgNPs developed from the reaction mixture have maxima between 400-450 nm. This hump-type peak in this range was due to the transition of electrons. These absorption spectra hinted that reduction was attained by applying CTAB. The reduction was exhibited by broadening the peak to indicate the synthesis of poly-dispersed AgNPs [16]. Spectra also showed the rapid synthesis of AgNPs, within 15 minutes, and their stability for three days.

3.3 Effect of pH

Further in the sequence, three different solutions of green AgNPs were adjusted to acidic, neutral, and basic pH by using 1N NaOH and simultaneously checked the UV-Vis spectra to confirm the stability of AgNPs. By increasing the pH of NPs solution height as well as absorbance of the peak increased. UV-Vis spectra of different pH green AgNPs solutions are shown in the same Figure 2. From this data, it is concluded that on increasing the height of the peaks, the size of the NPs also decreased [17].

At acidic pH, a small hump SPR peak was observed to indicate a small number of AgNPs. An increase in SPR peak intensities at basic and neutral pH indicated the increase of smaller AgNPs. A hump-shaped SPR peak denotes the uniform formation of AgNPs. A possible explanation for a higher number of green AgNPs at neutral and alkaline pH is the deposition of hydroxides on the AgNPs. At basic pH, both capping and reducing agents reduce the particles. Capping takes place at particular facets. This capping favors the formation of spherical NPs. At acidic pH, all functional groups that are accountable for the bio-formation of NPs acquired positive (+ve) charge. Due to this NPs are not sufficiently stable to stop agglomeration. The reducing capability of functional groups increases from acidic pH to basic pH for the synthesis of the thermodynamically suitable shape of NPs. In this work, it is observed that low pH suppressed the synthesis of AgNPs and high pH increased the synthesis of AgNPs [18].

3.4 Transmission electron microscopy (TEM)

Figure 3 (a, b and c) shows the size and surface structure of developed AgNPs. Images exhibited the particle size range is 10-20 nm with dispersive spherical morphology. Few aggregates of nanoparticles were observed.

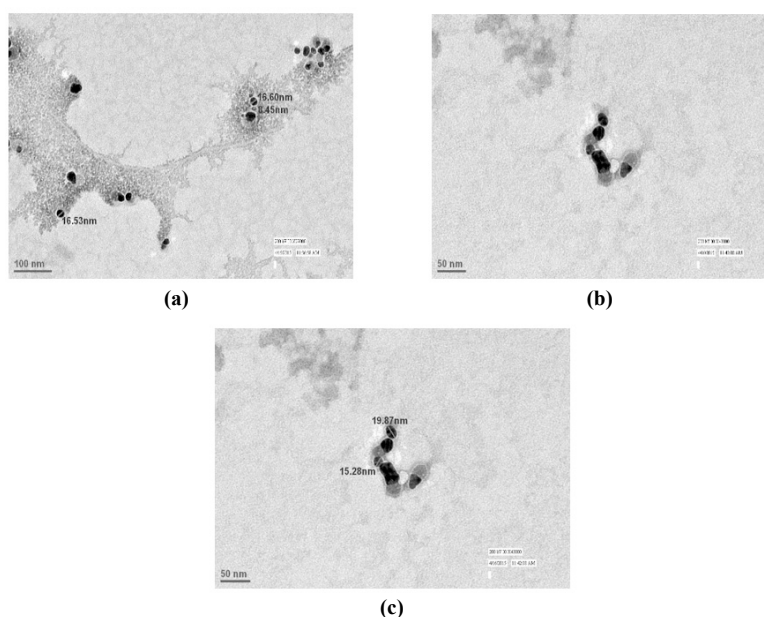


Figure 3. TEM image of Ag nanoparticles

3.5 Fourier transform infrared spectroscopy (FTIR)

The changes in FTIR peaks observe the encapsulation of AgNPs into the optimized hydrogel. From Figure 4, the peak at $1,320\text{ cm}^{-1}$ was of the acetyl group of CS [19] in CP1 hydrogel film which moved slightly towards lower frequency in CPAg.

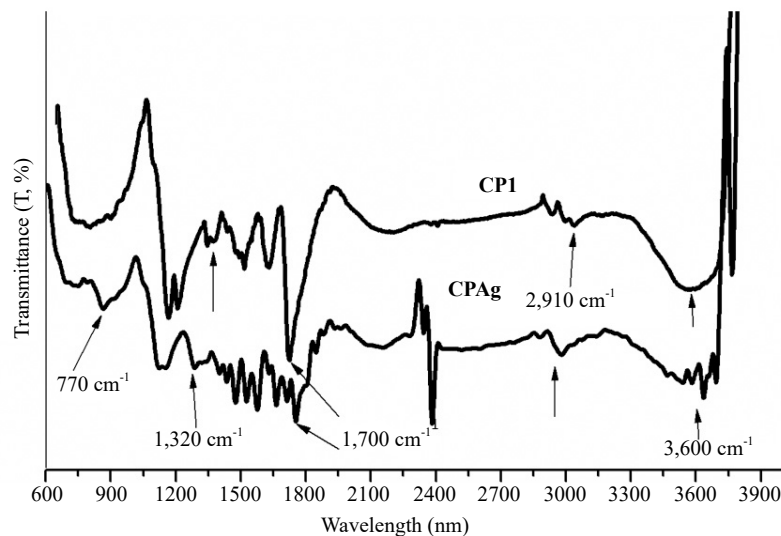


Figure 4. FTIR of chitosan/pNIPAm optimized hydrogel in 1:3 ratio (CP3) optimized hydrogel film and CPAg

The peak at $\sim 1,700\text{ cm}^{-1}$ was of $>\text{C}=\text{O}$ of PVP in CP1 moved slightly higher frequency in the case of CPAg designating that AgNPs get linked to the functional groups in CP1 which were shown by arrows in Figure 4. Interestingly, the position of CH_2 asymmetric stretching vibrations and $\text{C}-\text{H}$ bond of CP1 chains at $\sim 3,000\text{ cm}^{-1}$ [20] remain as such but the intensity of this peak increased in the case of CPAg which certified that the loading of AgNPs could increase the stretching and flexibility of CPAg [21]. The peak at 770 cm^{-1} was of AgNPs peaks in CPAg which showed the presence of AgNPs in the CPAg. As referenced in previous studies the zinc oxide (ZnO) nanoparticles peak in CS-based hydrogel was also present at 510 cm^{-1} but the AgNPs peak was slightly high [22]. The absence of the $1,568\text{ cm}^{-1}$ peak that was present in CP1 and the generation of one more peak at $1,724\text{ cm}^{-1}$ signify the interaction of AgNPs to the hydrogel. The displacement of the peak is due to coordinate bond formation between Ag and electron-rich groups like oxide (O) and nitrogen (N), in the hydrogel [23]. This interaction causes an enhancement in bond length and finally shifting of peaks.

3.6 Field emission scanning electron microscopy (FESEM)

The morphology of CP1 hydrogel is already discussed in our previous study [11]. The CP1 hydrogel was clear to the naked eye. Images do not exhibit any kind of phase separation and precipitation. CP1 was smooth and even. CP1 hydrogel film was porous as mentioned by three-dimensional (3D) images in our previous study [20]. The addition of pNIPAm appeared as a circular interactive network from the surface of CP1. FESEM images from Figure 5 (a, b and c) easily show encapsulated extract into the CP1 hydrogel films in the form of square and triangular shapes.

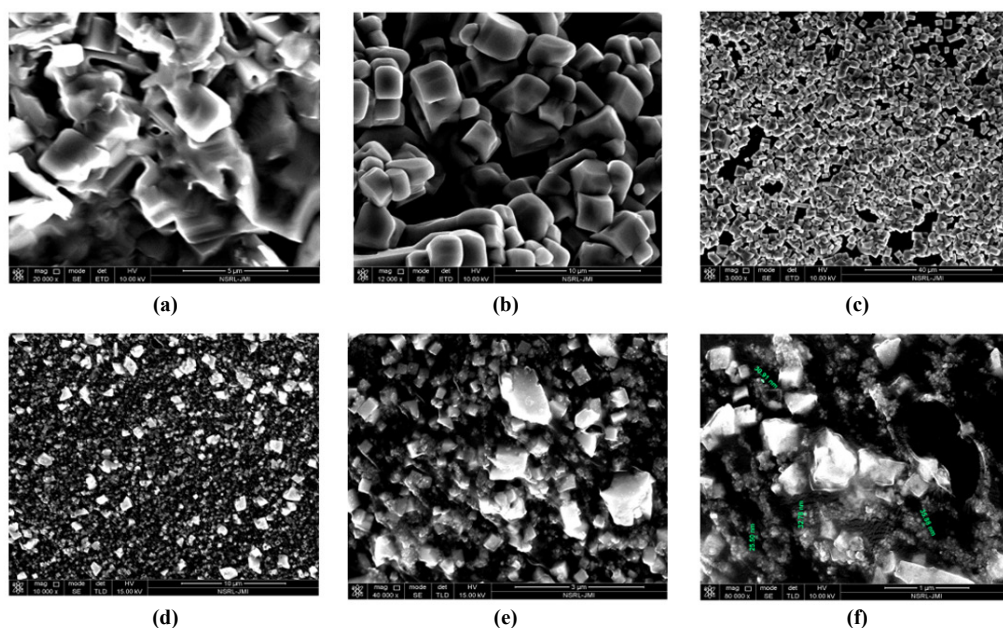


Figure 5. FESEM results: (a, b and c) extract loaded hydrogel film and (d, e and f) CPAG showing loading of Ag nanoparticles

Figure 5 (a and b) is the magnified images of only extract-loaded hydrogel films but Figure 5 (d, e and f) is the AgNPs loaded images of CPAG which showed NPs as well as unreacted triangular and square shape extract. From these images, it is confirmed that hydrogel films absorb both AgNPs as well as an unreacted extract from the NPs colloidal solution at different pH and at different temperatures. From Figure 5(f), on very high magnification, AgNPs are seen to be uniformly distributed and embedded with a size range of 25-36 nm into the CPAG films. Encapsulated AgNPs size increased by ~20 nm. A notable amount of increase in size of AgNPs after encapsulation into the CPAG hydrogel may be due to the participation of oxidation and balancing of stabilization process by polymeric chains.

3.7 Antibacterial assay

Evaluation of the antibacterial activity of CPAG hydrogel samples, 2x2 cm, by disc diffusion process against *E. coli* shown in Table 1 at pH 4.4, 7.4, 9.4 of 25 °C and 37 °C.

Table 1. Area of the zone of inhibition of CPAG against *E. coli*

No.	pH of the solution	Zone of inhibition at 25 °C	Zone of inhibition at 37 °C
1	4.4	17 mm	13 mm
2	7.4	13 mm	10 mm
3	9.4	12 mm	7 mm

It was found that pH 4.4, 7.4, and 9.4 colloidal solutions, NPs loaded CPAG hydrogel samples showed the inhibition zone against *E. coli* at 25 °C as 17 mm, 13 mm and 12 mm respectively. Whereas, CPAG hydrogel samples of pH 4.4, 7.4, and 9.4 colloidal solutions NPs of 37 °C showed zone of inhibitions 13 mm, 10 mm and 7 mm, respectively. At 25 °C hydrophilicity of pNIPAm facilitate the absorption of AgNPs into CP1 hydrogel film but at an increasing temperature of 37 °C pNIPAm becomes hydrophobic which absorbs more H₂O but not AgNPs [11]. From increasing temperature, H₂O easily penetrates the open chains of the hydrogel but the passage of the chain was not enough for AgNPs absorption. So, upon increasing the temperature from 25 °C to 37 °C the absorption of AgNPs from every

solution and area of the zone of inhibition decreased. As we know the phase transition of pNIPAm from hydrophilic to hydrophobic above its >lower critical solution temperature (LCST) (32 °C) would not allow AgNPs into CPAG and which would also affect the absorption of AgNPs into the hydrogel films. From Table 1 moving from upwards to downwards the area of the zone of inhibition decreased in every case of 25 °C and 37 °C of CPAG samples because the major portion of the CPAG hydrogel was of CS which is pH sensitive. At pH 4.4, protonation of the NH₂ group of CS into NH₃⁺ [24] takes place due to which repulsion of CPAG hydrogel chains takes place which facilitates the opening and absorption of AgNPs into CPAG. So, at pH 4.4, the zone of inhibition was very high and the zone of inhibition was very least in the case of pH 9.4 CPAG case. From these results, we clearly realize that CPAG hydrogel exhibits excellent antimicrobial activity.

4. Conclusion

Biologically active wound dressings can be considered an emerging option that could have a significant impact on the life of people. The nanoparticles were synthesized by a green route which is found to be efficient in comparison to the conventional methods. The presence of AgNPs in the hydrogel was confirmed via FESEM, TEM and FTIR. Hydrogels exhibit excellent antimicrobial activity against *E. coli* and can be used in wound care. The antibacterial experiment indicated that the hydrogel of CS/PVP/PNIPAm loaded with AgNPs had good bactericidal activity against the Gram-negative bacteria *E. coli*, and these hydrogels might be useful in caring for wounds.

Acknowledgement

The authors would want to offer their appreciation to colleagues for their attempt in making the initial draft of this article.

Conflict of interest

The authors declare that they have no conflict of interest.

References

- [1] Khan I, Saeed K, Khan I. Nanoparticles: Properties, applications and toxicities. *Arabian Journal of Chemistry*. 2019; 12(7): 908-931. <https://doi.org/10.1016/j.arabjc.2017.05.011>
- [2] Kalan L, Grice EA. Fungi in the wound microbiome. *Advances in Wound Care*. 2018; 7(7): 247-255. <https://doi.org/10.1089/wound.2017.0756>
- [3] Gour A, Jain NK. Advances in green synthesis of nanoparticles. *Artificial Cells, Nanomedicine, and Biotechnology*. 2019; 47(1): 844-851. <https://doi.org/10.1080/21691401.2019.1577878>
- [4] Urnukhsaikhan E, Bold B-E, Gunbileg A, Sukhbaatar N, Mishig-Ochir T. Antibacterial activity and characteristics of silver nanoparticles biosynthesized from *Carduus crispus*. *Scientific Reports*. 2021; 11: 21047. <https://doi.org/10.1038/s41598-021-00520-2>
- [5] Jayaprakash N, Vijaya JJ, Kaviyarasu K, Kombaiiah K, Kennedy LJ, Ramalingam RJ, et al. Green synthesis of Ag nanoparticles using Tamarind fruit extract for the antibacterial studies. *Journal of Photochemistry and Photobiology B: Biology*. 2017; 169: 178-185. <https://doi.org/10.1016/j.jphotobiol.2017.03.013>
- [6] Dadashpour M, Firouzi-Amandi A, Pourhassan-Moghaddam M, Maleki MJ, Soozangar N, Jeddi FM, et al. Biomimetic synthesis of silver nanoparticles using *Matricaria chamomilla* extract and their potential anticancer activity against human lung cancer cells. *Materials Science and Engineering: C*. 2018; 92(1): 902-912. <https://doi.org/10.1016/j.msec.2018.07.053>
- [7] Wang P, Zhang Z, Wang L, Fan S, Deng Y, Liang Q, et al. Synthesis of superabsorbent polymer hydrogels with rapid swelling: Effect of reaction medium dosage and polyvinylpyrrolidone on water absorption rate. *Langmuir*.

- 2021; 37(50): 14614-14621. <https://doi.org/10.1021/acs.langmuir.1c02295>
- [8] Pellá MCG, Lima-Tenório MK, Tenório-Neto ET, Guilherme MR, Muniz EC, Rubira AF. Chitosan-based hydrogels: From preparation to biomedical applications. *Carbohydrate Polymers*. 2018; 196: 233-245. <https://doi.org/10.1016/j.carbpol.2018.05.033>
- [9] Rasool A, Ata S, Islam A. Stimuli responsive biopolymer (chitosan) based blend hydrogels for wound healing application. *Carbohydrate Polymers*. 2019; 203: 423-429. <https://doi.org/10.1016/j.carbpol.2018.09.083>
- [10] Liu P, Song L, Li N, Lin J, Huang D. Time dependence of phase separation enthalpy recovery behavior in aqueous poly (N-isopropylacrylamide) solution. *Journal of Thermal Analysis and Calorimetry*. 2017; 130: 843-850. <https://doi.org/10.1007/s10973-017-6460-8>
- [11] Qureshi MA, Khatoon F. In vitro study of temperature and pH-responsive gentamycin sulphate-loaded chitosan-based hydrogel films for wound dressing applications. *Polymer-Plastics Technology and Engineering*. 2015; 54(6): 573-580. <https://doi.org/10.1080/03602559.2014.974186>
- [12] Serati-Nouri H, Jafari A, Roshangar L, Dadashpour M, Pilehvar-Soltanahmadi Y, Zarghami N. Biomedical applications of zeolite-based materials: A review. *Materials Science and Engineering: C*. 2020; 116: 111225 <https://doi.org/10.1016/j.msec.2020.111225>
- [13] Nejati K, Dadashpour M, Gharibi T, Mellatyar H, Akbarzadeh A. Biomedical applications of functionalized gold nanoparticles: A review. *Journal of Cluster Science*. 2021; 33: 1-16. <https://doi.org/10.1007/s10876-020-01955-9>
- [14] Mlalila NG, Swai HS, Hilonga A, Kadam DM. Antimicrobial dependence of silver nanoparticles on surface plasmon resonance bands against *Escherichia coli*. *Nanotechnology Science and Applications*. 2017; 10: 1-9. <https://doi.org/10.2147/NSA.S123681>
- [15] Namratha N, Monica PV. Synthesis of silver nanoparticles using *Azadirachta indica* (Neem) extract and usage in water purification. *Asian Journal of Pharmacy and Technology*. 2013; 3(4): 170-174. <https://www.indianjournals.com/ijor.aspx?target=ijor:ajpt&volume=3&issue=4&article=008>
- [16] Selvakumar P, Sithara R, Viveka K, Sivashanmugam P. Green synthesis of silver nanoparticles using leaf extract of *Acalypha hispida* and its application in blood compatibility. *Journal of Photochemistry and Photobiology B: Biology*. 2018; 182: 52-61. <https://doi.org/10.1016/j.jphotobiol.2018.03.018>
- [17] Maria BS, Devadiga A, Kodialbail VS, Saidutta MB. Synthesis of silver nanoparticles using medicinal *Zizyphus xylopyrus* bark extract. *Applied Nanoscience*. 2015; 5: 755-762. <https://doi.org/10.1007/s13204-014-0372-8>
- [18] Traiwatcharanon P, Timsorn K, Wongchoosuk C. Effect of pH on the green synthesis of silver nanoparticles through reduction with *Pistiastratiotes L.* extract. In: *Advanced materials research*. Switzerland: Trans Tech Publications; 2016. p.223-226.
- [19] Dennis G, Harrison W, Agnes K, Erastus G. Effect of biological control antagonists adsorbed on chitosan immobilized silica nanocomposite on *Ralstonia solanacearum* and growth of tomato seedlings. *Advances in Research*. 2016; 6(3): 1-23. <https://doi.org/10.9734/AIR/2016/22742>
- [20] Qureshi MA, Khatoon F, Rizvi MA, Zafaryab M. Ethyl acetate *Salix alba* leaves extract-loaded chitosan-based hydrogel film for wound dressing applications. *Journal of Biomaterials Science, Polymer Edition*. 2015; 26: 1452-1464. <https://doi.org/10.1080/09205063.2015.1100843>.
- [21] Agnihotri S, Mukherji S, Mukherji S. Antimicrobial chitosan-PVA hydrogel as a nanoreactor and immobilizing matrix for silver nanoparticles. *Applied Nanoscience*. 2012; 2: 179-188. <https://doi.org/10.1007/s13204-012-0080-1>
- [22] Kumar PTS, Lakshmanan V-K, Anilkumar TV, Ramya C, Reshmi P, Unnikrishnan AG, et al. Flexible and microporous chitosan hydrogel/nano ZnO composite bandages for wound dressing: In vitro and in vivo evaluation. *ACS Applied Materials and Interfaces*. 2012; 4(5): 2618-2629. <https://doi.org/10.1021/am300292v>
- [23] Vimala K, Yallapu MM, Varaprasad K, Reddy NN, Ravindra S, Naidu NS, et al. Fabrication of curcumin encapsulated chitosan-PVA silver nanocomposite films for improved antimicrobial activity. *Journal of Biomaterials and Nanobiotechnology*. 2011; 2(1): 55-64. <https://doi.org/10.4236/jbnb.2011.21008>
- [24] Qureshi MA, Khatoon F. Development of citric acid cross linked poly(vinyl alcohol) hydrogel film, its degradability and effect of temperature, pH. *Advanced Science Letters*. 2014; 20(7-9): 1414-1419(6). <https://doi.org/10.1166/asl.2014.5546>